



# ANALYTICAL DESCRIPTION AND OPTIMIZATION OF THE DYNAMIC BEHAVIOUR OF PASSIVELY SUSPENDED ROAD VEHICLES

M. GOBBI AND G. MASTINU

*Department of Mechanical Engineering, Politecnico di Milano (Technical University),  
Piazza Leonardo da Vinci, 32, I-20133 Milan, Italy.  
E-mail: [gobbi@mecc.polimi.it](mailto:gobbi@mecc.polimi.it)*

*(Received 13 June 2000, and in final form 22 November 2000)*

A simple two-degree-of-freedom linear model is used to derive a number of analytical formulae describing the dynamic behaviour of passively suspended vehicles running on randomly profiled roads. Two different power spectral densities are considered for modelling the road irregularity. The derived analytical formulae can be used either during preliminary design or for other special purposes, especially when approximated results are acceptable.

An optimization method, based on Multi-Objective Programming and Monotonicity analysis, is introduced and applied for the symbolic derivation of analytical formulae featuring the best compromise among conflicting performance indices pertaining to the vehicle suspension system, i.e., discomfort, road holding and working space. The optimal settings of the relevant vehicle suspension parameters (i.e., tyre radial stiffness, spring stiffness and damping) are derived either symbolically and/or numerically.

© 2001 Academic Press

## 1. INTRODUCTION

In this paper the dynamic response of road vehicles running on rough roads is dealt with by deriving simple analytical formulae. This is useful for academic purposes but also for designers who may benefit from a simplified but general theory. In addition to the study of the dynamic response, the optimization of vehicle parameters is performed on the basis of Multi-Objective Programming, (MOP) a branch of Operations Research. The analytical formulae derived in the first part of the paper are used in conjunction with MOP to find symbolically the optimal suspension parameters ensuring the best compromise between discomfort (i.e., the standard deviation of the vehicle body vertical acceleration), road holding (i.e., the standard deviation of the vertical force applied between tyre and road) and body–wheel working space (i.e., the standard deviation of the relative displacement between wheel and vehicle body).

In the literature, a number of papers exist dealing with the problem of deriving simple analytical formulae for the estimation of the dynamic response of road vehicles subject to random excitations generated by road irregularity [1–6]. In each of the cited papers the derived formulae refer to a very simple power spectral density of road irregularity (of the form  $1/\omega^2$  [7]). Here a more complex power spectral density (of the form  $1/(\omega^2 + s_c^2)$ ) is used which estimates more accurately the amplitudes of the road irregularity at low excitation frequencies.

With reference to wheel and body vibrations, a number of authors have dealt with the problem of deriving basic concepts useful for road vehicle suspension tuning [3, 8–15]. Many important relationships have been highlighted among vehicle suspension parameters and suspension performance indices. However, an ultimate general theory was not derived. This was mainly due to the fact that a theoretical definition of the best compromise between conflicting performance indices was not explicitly introduced and properly exploited. Another limitation was that authors often resorted to numerical simulations even when dealing with simple models.

In this paper, an attempt to introduce a comprehensive general theory is performed by deriving analytical formulae defining the optimal relationship among vehicle suspension parameters and suspension performance indices. The derivation of these analytical formulae has been made possible by exploiting Multi-Objective Programming (MOP). MOP represents a rigorous theoretical way for selecting parameters when a number of conflicting requirements on system's performances have to be satisfied. In references [16–25] the adoption of MOP has been proposed to solve many engineering problems, with particular reference to vehicles. Basically, the optimization procedures based on MOP allow the best trade-off among user-defined conflicting performance indices to be found. Given the model, the designer is often charged with the hard task of finding *one optimal solution* by changing a number of parameters. When many performance indices have to be taken into account at the same time, and many parameters may be changed, often the optimization problem cannot be handled easily, i.e., a solution cannot be found in a straightforward way. Moreover, in this case, the concept of *optimal solution* is not obvious and requires a special definition (see e.g. reference [17]). The concept of optimal solution which will be considered may be synthesized by stating that if more than one criterion (performance index) has to be satisfied by changing one or more parameters, the possible optimal solutions constitute a set. This implies that the designer has to choose a preferred solution among those solutions (and only those) belonging to the set. As the solutions of the set are directly related to performance indices, the task of the designer is to consider performance indices (or criteria) instead of considering parameters. The methods (and related computer programs) that allow such a procedure (and thinking) are presented or reviewed in references [17–19]. Successful applications of the method in the field of ground vehicle design are reported in references [16, 21–26].

In the first part of the paper, analytical formulae describing the motions of road vehicles on rough road are derived. These formulae are used in the second part of the paper for deriving, by means of Multi-Objective Programming, the optimal tuning of the vehicle suspension parameters.

## 2. SYSTEM MODEL

### 2.1. EQUATIONS OF MOTION AND RESPONSE TO STOCHASTIC EXCITATION

The adopted quarter-car system model is shown in Figure 1. The mass  $m_1$  represents approximately the mass of the wheel plus part of the mass of the suspension arms,  $m_2$  represents approximately 1/4 of the body mass ( $m_2$  could be computed more precisely taking into account the position of the centre of gravity along the wheelbase, as shown in references [4, 8]). The excitation comes from the road irregularity  $\xi$ . The model is generally reputed to be sufficiently accurate for capturing the essential features related to discomfort, road holding and working space (see reference [8]). The linear equations of motions of the

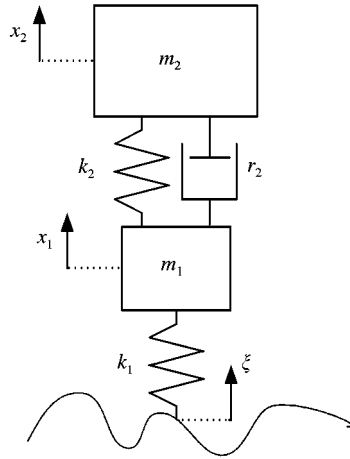


Figure 1. Quarter car vehicle model.

system model are

$$\begin{aligned}
 m_1\ddot{x}_1 - r_2(\dot{x}_2 - \dot{x}_1) - k_2(x_2 - x_1) + k_1(x_1 - \xi) &= 0, \\
 m_2\ddot{x}_2 + r_2(\dot{x}_2 - \dot{x}_1) + k_2(x_2 - x_1) &= 0.
 \end{aligned}
 \tag{1}$$

The responses of the vehicle model are, respectively, the vertical vehicle body acceleration ( $\ddot{x}_2$ ), the force applied between road and wheel ( $F_{z1}$ ), the relative displacement between wheel and vehicle body ( $x_2 - x_1$ ).

The discomfort is evaluated by computing the standard deviation of the vertical vehicle body acceleration ( $\sigma_{\ddot{x}_2}$ ). The higher the standard deviation, the higher is the *discomfort*. This approach seems to provide very good correlation with subjective ride comfort ratings [2, 27].

The standard deviation of the tyre radial force ( $\sigma_{F_z}$ ) is related to *road holding*. The variation of tyre radial force can lead to a loss of contact with the ground and poor handling ability [2].

The standard deviation of the relative displacement between the wheel and vehicle body ( $\sigma_{x_2 - x_1}$ ), i.e., the rattle space or *working space*, is related to design and packaging constraints, as well as to wheel lateral vibrations.

Discomfort ( $\sigma_{\ddot{x}_2}$ ), road holding ( $\sigma_{F_z}$ ) and working space ( $\sigma_{x_2 - x_1}$ ) are the *performance indices* to which reference will be made in the paper.

The transfer function [25] between the displacement  $\xi$  and  $x_1$  is given by

$$X_1(j\omega) = \frac{k_1(k_2 + jr_2\omega - m_2\omega^2)}{D(j\omega)}, \tag{2}$$

$$\begin{aligned}
 D(j\omega) &= k_1k_2 + jk_1r_2\omega - (k_2m_1 + k_1m_2 + k_2m_2)\omega^2 \\
 &\quad - jr_2(m_1 + m_2)\omega^3 + m_1m_2\omega^4.
 \end{aligned}$$

The transfer function between the imposed displacement  $\xi$  and  $x_2$  is

$$X_2(j\omega) = \frac{k_1(k_2 + jr_2\omega)}{D(j\omega)}. \quad (3)$$

The transfer function between  $\xi$  and  $\ddot{x}_2$  is

$$H_1(j\omega) = -\omega^2 X_2(j\omega). \quad (4)$$

The transfer function between  $\xi$  and  $F_{z1}$  is

$$H_2(j\omega) = k_1(1 - X_1(j\omega)). \quad (5)$$

The transfer function between  $\xi$  and  $x_2 - x_1$  is

$$H_3(j\omega) = X_2(j\omega) - X_1(j\omega). \quad (6)$$

The displacement  $\xi$  (road irregularity) may be represented by a random variable defined by a stationary and ergodic stochastic process with zero mean value [7, 28]. The power spectral density (PSD) of the process may be determined on the basis of experimental measurements and in the literature there are many different formulations for it (e.g., see references [7, 9]).

In this paper, two spectra have been considered:

$$S_{\xi_1}(\omega) = \frac{A_b v}{\omega^2}, \quad (7)$$

$$S_{\xi_2}(\omega) = \frac{A_v s_c}{(s_c^2 + \omega^2)}, \quad (8)$$

where  $s_c = av$ . The value of the coefficient  $a$  (rad/m) depends on the shape of the road irregularity spectrum.

In a log-log scaled plot (abscissa  $\omega$ ), the spectrum of equation (7) takes the shape of a line sloped at rate  $-2$ . The simple expression (7) approximates various roads with different degrees of accuracy. It generally overestimates the amplitudes of the irregularity at low frequency. In the following, equation (7) will be shown as *one slope* power spectral density (1S-PSD).

A better correlation with measured spectra can be obtained by resorting to more complex spectra as suggested in reference [7]. Equation (8) has been reported in references [9, 29]. In a log-log scaled plot (abscissa  $\omega$ ) equation (8) takes the shape of a *two slope curve*, thus reference will be made by the acronym 2S-PSD.

The parameters  $A_b$  and  $A_v$  are obviously uncorrelated as they refer to two different excitation spectra.

The power spectral density (PSD)  $S_l$  of the output of an asymptotically stable system can be computed as (see, e.g., reference [1])

$$S_l(\omega) = |H_l(j\omega)|^2 S_{\xi_q}(\omega), \quad l = 1, \dots, 3, \quad q = 1, 2. \quad (9)$$

For  $l = 1$ ,  $S_l$  represents the PSD of the vertical acceleration of the vehicle body, for  $l = 2$ ,  $S_l$  represents the PSD of the vertical force at the wheel-road interface, and for  $l = 3$ ,  $S_l$  represents the PSD of the relative displacement chassis-wheel (suspension stroke), the index  $q = 1$  refers to the 1S-PSD and the index  $q = 2$  refers to the 2S-PSD.

2.2. DERIVATION OF STANDARD DEVIATIONS IN ANALYTICAL FORM

By definition (see reference [1]) the variance of a random variable described by a stationary and ergodic stochastic process is

$$\sigma_I^2 = \frac{1}{2\pi} \int_{-\infty}^{+\infty} S_I(\omega) d\omega. \tag{10}$$

In reference [30] it is shown that an analytical solution exists for  $\sigma_I^2$  if  $S_I$  can be written as

$$S_I = \frac{N_{k-1}(j\omega)N_{k-1}(-j\omega)}{D_k(j\omega)D_k(-j\omega)}, \tag{11}$$

where  $D_k$  is a polynomial of degree  $k$ , and  $N_{k-1}$  is a polynomial of degree  $k - 1$  ( $k \geq 1$ ). By inspection of equations (4-9) one may understand that  $S_I$  can be written as in equation (11); in fact, for example, considering the vertical acceleration of the vehicle body ( $\ddot{x}_2$ ), and being, from equation (9)

$$S_1(\omega) = |H_1(j\omega)|^2 S_{\xi q}(j\omega), \quad q = 1, 2$$

and being

$$|H_1(j\omega)|^2 = H_1(j\omega)H_1(-j\omega)$$

and, for  $q = 1$

$$S_{\xi 1}(\omega) = \frac{A_b v}{\omega^2} \rightarrow S_{\xi 1}(j\omega) = A_b v \frac{1}{j\omega} \frac{1}{(-j\omega)}$$

and, for  $q = 2$

$$S_{\xi 2}(\omega) = \frac{A_v s_c}{(s_c^2 + \omega^2)} \rightarrow S_{\xi 2}(j\omega) = A_v s_c \frac{1}{(s_c + j\omega)} \frac{1}{(s_c - j\omega)},$$

the following expressions for  $N_{k-1}(j\omega)/D_k(j\omega)$  can be obtained: for  $q = 1$  (1S-PSD),  $k = 4$  (see equations (3, 4))

$$\begin{aligned} & \frac{N_2(j\omega)}{D_4(j\omega)} \\ &= (A_b v)^{1/2} \frac{k_1 j\omega(k_2 + r_2 j\omega)}{(k_1 k_2 + j k_1 r_2 \omega - (k_2 m_1 + k_1 m_2 + k_2 m_2)\omega^2 - j r_2(m_1 + m_2)\omega^3 + m_1 m_2 \omega^4)} \end{aligned}$$

for  $q = 2$ , (2S-PSD),  $k = 5$  (see equations (3, 4)).

$$\begin{aligned} & \frac{N_3(j\omega)}{D_5(j\omega)} \\ &= (A_b s_c)^{1/2} \frac{-k_1 \omega^2(k_2 + r_2 j\omega)}{[k_1 k_2 + j k_1 r_2 \omega - (k_2 m_1 + k_1 m_2 + k_2 m_2)\omega^2 - j r_2(m_1 + m_2)\omega^3 + m_1 m_2 \omega^4] (j\omega + s_c)}. \end{aligned}$$

It is important to notice that  $S_l$  can be written as in equation (11) if  $S_{\xi q}(j\omega)$  can be expressed as

$$S_{\xi q}(j\omega) = \frac{N_{\xi}(j\omega)N_{\xi}(-j\omega)}{D_{\xi}(j\omega)D_{\xi}(-j\omega)}.$$

This occurrence was first exploited in reference [4], with reference to the simple 1S-PSD ( $q = 1$ ). The more refined 2S-PSD ( $q = 2$ ) has been introduced in this paper.

The analytical formulae presented in the following subsections have been derived by means of the analytical solutions of integral (10) introduced in reference [30] and reported in Appendix A.

2.2.1. *Formulae referring to the 1S-PSD (equation (7))*

The analytical formulae giving the discomfort, road holding and working space are reported. They have been obtained by solving analytically equation (10) (1S-PSD).  
 —Variance of the vehicle body acceleration  $\ddot{x}_2$  (square of  $\sigma_{\ddot{x}_2}$ )

$$\sigma_{\ddot{x}_2}^2 = 1/2 A_b v \bar{\sigma}_{\ddot{x}_2}^2, \tag{12}$$

$$\bar{\sigma}_{\ddot{x}_2}^2 = \frac{1}{m_2^2} \left( \frac{(m_2 + m_1)k_2^2}{r_2} + k_1 r_2 \right). \tag{13}$$

— Variance of the force acting between road and wheel  $F_z$  (square of  $\sigma_{F_z}$ )

$$\sigma_{F_z}^2 = 1/2 A_b v \bar{\sigma}_{F_z}^2, \tag{14}$$

$$\bar{\sigma}_{F_z}^2 = (m_2 + m_1)^2 (P), \tag{15}$$

$$P = \left( \frac{(m_2 + m_1)k_2^2}{m_2^2 r_2} - \frac{2k_1 k_2 m_1}{m_2 r_2 (m_2 + m_1)} + \frac{k_1^2 m_1}{r_2 (m_2 + m_1)^2} + \frac{k_1 r_2}{m_2^2} \right).$$

—Variance of the relative displacement between wheel and vehicle body  $x_2 - x_1$  (square of  $\sigma_{x_2 - x_1}$ )

$$\sigma_{x_2 - x_1}^2 = 1/2 A_b v \bar{\sigma}_{x_2 - x_1}^2, \tag{16}$$

$$\bar{\sigma}_{x_2 - x_1}^2 = \frac{(m_2 + m_1)}{r_2}. \tag{17}$$

These formulae were already derived and presented in references [3, 4, 5, 25].

Figure 2 shows, respectively, the discomfort ( $\sigma_{\ddot{x}_2}$ ), road holding ( $\sigma_{F_z}$ ) and working space ( $\sigma_{x_2 - x_1}$ ) as function of the vehicle speed ( $v$ ) considering the reference vehicle.

2.2.2. *Formulae referring to the 2S-PSD (equation (8))*

The analytical formulae giving the discomfort, road holding and working space are reported. They have been obtained by solving analytically equation (10) (2S-PSD).

—Variance of the vehicle body acceleration  $\ddot{x}_2$  (square of  $\sigma_{\ddot{x}_2}$ )

$$\sigma_{\ddot{x}_2}^2 = c_{rv} \frac{[k_1^2 r_2^2 (k_2 + r_2 s_c + m_2 s_c^2) + k_1 k_2^2 ((m_1 + m_2) (k_2 + r_2 s_c) + m_1 m_2 s_c^2)]}{(m_2^2 r_2 (D_s))}, \tag{18}$$

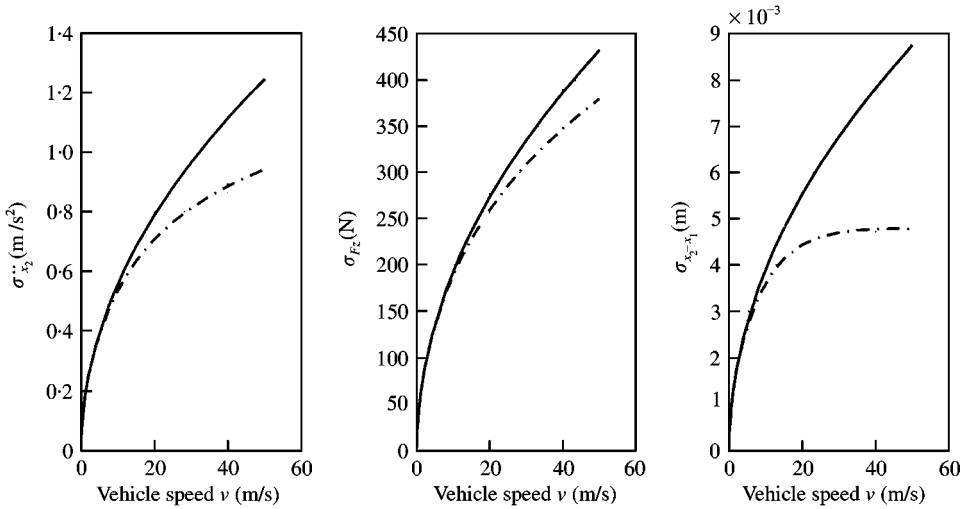


Figure 2. Discomfort ( $\sigma_{\dot{x}_2}$ ), road holding ( $\sigma_{F_z}$ ), working space ( $\sigma_{x_2-x_1}$ ) as function of the vehicle speed. Data of the reference vehicle in Table 1, running condition data in Table 2. —, 1S-PSD; - - - - - , 2S-PSD.

where

$$D_S = k_1 k_2 + k_1 r_2 s_c + k_2 (m_1 + m_2) s_c^2 + k_1 m_2 s_c^2 + (m_1 + m_2) r_2 s_c^3 + m_1 m_2 s_c^4,$$

$$s_c = av, \quad c_{rv} = 1/2 A_v av.$$

—Variance of the force acting between road and wheel  $F_z$  (square of  $\sigma_{F_z}$ )

$$\sigma_{F_z}^2 = c_{rv} \frac{(A_{2S} + B_{2S} + C_{2S})}{k_1^2 m_2^2 r_2^2 (D_S)}, \tag{19}$$

where

$$A_{2S} = k_1^4 (m_1 + m_2) r_2 (-2k_2 m_1 m_2 + m_1 r_2^2 + m_2 r_2^2) (k_2 + r_2 s_c + m_2 s_c^2),$$

$$B_{2S} = k_1^3 k_2^2 (m_1 + m_2)^2 r_2 (k_2 m_1 + k_2 m_2 + m_1 r_2 s_c + m_2 r_2 s_c + m_1 m_2 s_c^2),$$

$$C_{2S} = k_1^4 m_1 m_2^2 r_2 (k_1 k_2 + k_1 r_2 s_c + k_1 m_2 s_c^2 + k_2 m_2 s_c^2 + m_2 r_2 s_c^3).$$

—Variance of the relative displacement between wheel and vehicle body  $x_2 - x_1$  (square of  $\sigma_{x_2-x_1}$ )

$$\sigma_{x_2-x_1}^2 = c_{rv} \frac{k_1 (k_2 m_1 + k_2 m_2 + m_1 r_2 s_c + m_2 r_2 s_c + m_1 m_2 s_c^2)}{r_2 (D_S)}. \tag{20}$$

The main difference between the formulae referring to the 1S-PSD (equation (12–17)) and those referring to 2S-PSD (equation (18–20)) is that in the first formulae the running condition parameters  $A_b$  and  $v$  are always not mixed with system model parameters ( $m_1, m_2, k_1, k_2, r_2$ ). The opposite occurs for 2S-PSD formulae in which running condition parameters  $s_c, c_{rv}$  are mixed with model parameters ( $m_1, m_2, k_1, k_2, r_2$ ). This implies that for 1S-PSD excitation, the minima of  $\sigma_{\dot{x}_2}, \sigma_{F_z}, \sigma_{x_2-x_1}$  (as function of the suspension parameters) do not depend on running conditions ( $A_b, v$ ).

## 2.3. PARAMETER SENSITIVITY ANALYSIS

The dynamic response of the road vehicle system model in Figure 1 is analyzed on the basis of equations (12, 14, 16, 18–20). A typical, small-sized sports car is taken into consideration (vehicle data in Table 1 and road roughness data in Table 2). All graphical results in the paper refer to this vehicle, and thus they do not have a general meaning and might even be qualitatively inaccurate for another (quite different) vehicle. However, the formulae derived in the previous paragraph do have a general meaning and can be used for simulating the comfort, road holding and working space of every road vehicle that could be modelled as in Figure 1.

The results of the parameter sensitivity analysis are shown in Figures 3–5. The parameters are varied within wide ranges. The data are presented in non-dimensional form, i.e., the standard deviation of interest  $\sigma_j$  is divided by the corresponding one ( $\sigma_{j_r}$ ) computed by considering the parameters at their reference values reported in Table 1, i.e.,

$$\sigma_{\ddot{x}_2 r} = \sigma_{\ddot{x}_2}(m_{1r}, m_{2r}, k_{1r}, k_{2r}, r_{2r}), \quad (21)$$

$$\sigma_{F_z r} = \sigma_{F_z}(m_{1r}, m_{2r}, k_{1r}, k_{2r}, r_{2r}), \quad (22)$$

$$\sigma_{x_2 - x_1 r} = \sigma_{x_2 - x_1}(m_{1r}, m_{2r}, k_{1r}, k_{2r}, r_{2r}), \quad (23)$$

The non-dimensional standard deviations given by equations (12, 14, 16) do not depend on vehicle speed. The opposite occurs for the non-dimensional standard deviations derived from equations (18–20) referring to excitation given by 2S-PSD (equation (8)). For this reason these non-dimensional standard deviations are analyzed at two different vehicle speeds, low speed (10 m/s) and high speed (50 m/s).

TABLE 1  
*Data of the reference road vehicle taken into consideration*

Parameter	Reference value	Lower and upper bound <sup>†</sup>
$m_{1r}$ (kg)	229	114–458
$m_{2r}$ (kg)	31	15–62
$k_{1r}$ (N/m)	120 000	60 000–240 000
$k_{2r}$ (N/m)	20 000	10 000–40 000
$r_{2r}$ (N s/m)	1200	600–2400

<sup>†</sup> Lower and upper bounds refer to parameter sensitivity analysis.

TABLE 2  
*Data of the road roughness taken into consideration*

Parameter	Reference value	
$A_b$	(m)	1.4e-5
$a = s_c/v$	(rad/m)	0.4
$A_v$	(m <sup>2</sup> )	3.5e-5



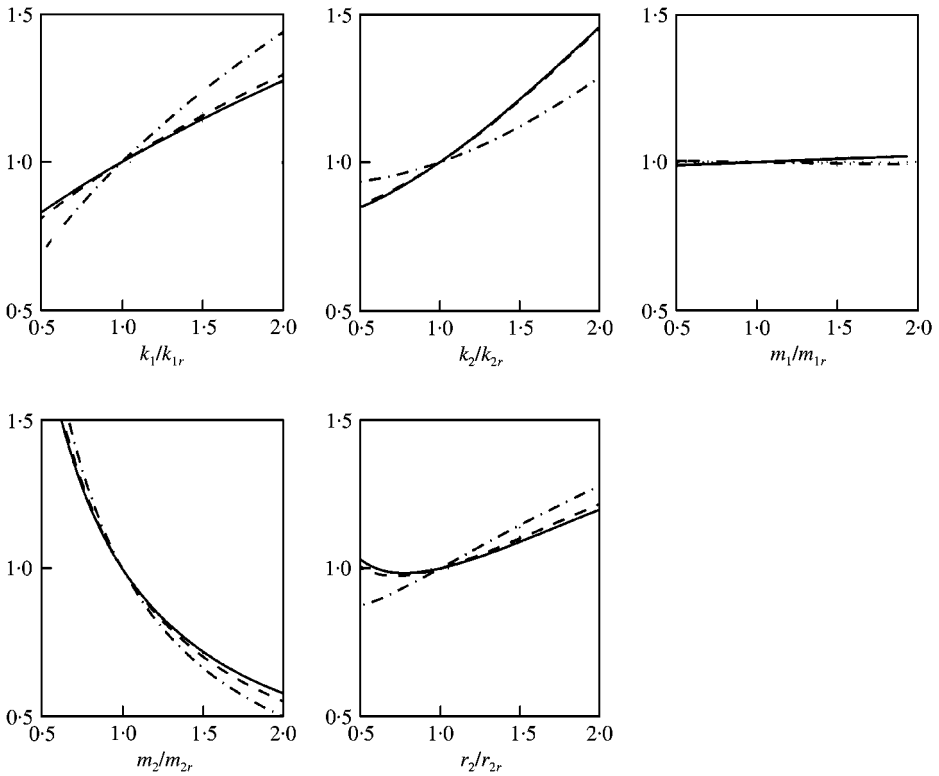


Figure 3.  $\sigma_{\ddot{x}_2}/\sigma_{\ddot{x}_2r}$ : non-dimensional standard deviation of the vertical body acceleration as function of model parameters. Data of the reference vehicle in Table 1, running condition data in Table 2. Each diagram has been obtained by varying one single parameter, the other ones being constant and equal to those of the reference vehicle. ---, 2S-PSD:  $v = 10$  m/s; ·-·-·, 2S-PSD:  $v = 50$  m/s; —, 1S-PSD: any speed.

2.3.1. Standard deviation of the vertical body acceleration (discomfort)

By inspection of Figure 3 it may be noted that

- (1) the tyre radial stiffness  $k_1$  influences significantly  $\sigma_{\ddot{x}_2}$  (the influence is stronger at high speed considering the 2S-PSD),
- (2)  $\sigma_{\ddot{x}_2}$  increases with the suspension stiffness  $k_2$ ,
- (3)  $\sigma_{\ddot{x}_2}$  does not depend significantly on the wheel mass  $m_1$ ,
- (4)  $\sigma_{\ddot{x}_2}$  depends strongly on the vehicle body mass  $m_2$ ,
- (5) the suspension damping  $r_2$  has influence on the standard deviation  $\sigma_{\ddot{x}_2}$ .

Some of the above considerations can be derived by inspection of equation (12) or equation (18).

2.3.2. Standard deviation of the dynamic wheel load (road holding)

Figure 4 shows that

- (1)  $\sigma_{F_z}$  depends linearly on the tyre stiffness  $k_1$ ,
- (2)  $\sigma_{F_z}$  increases with the suspension stiffness  $k_2$  (almost the opposite occurs at high speed considering the 2S-PSD),
- (3)  $\sigma_{F_z}$  increases with the wheel mass  $m_1$ ,

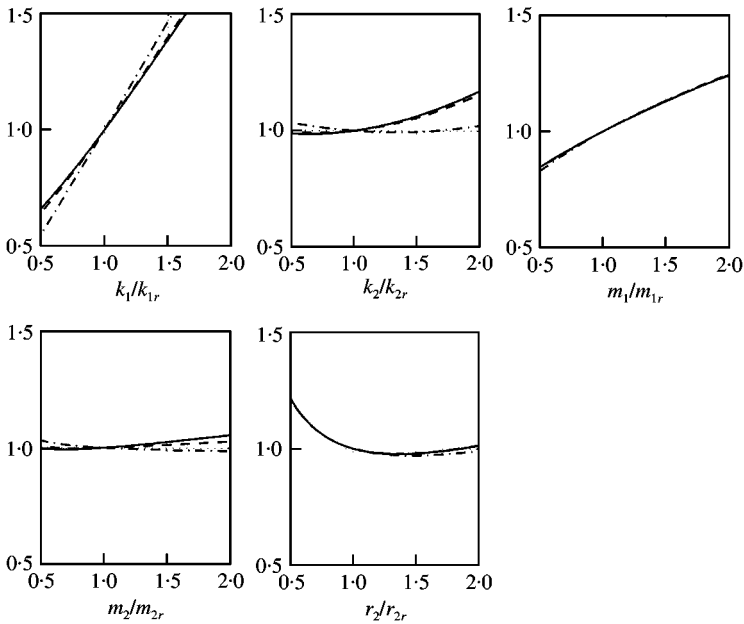


Figure 4.  $\sigma_{F_z}/\sigma_{F_z,r}$ : non-dimensional standard deviation of road holding as a function of model parameters. Data of the reference vehicle in Table 1, running condition data in Table 2. Each diagram has been obtained by varying one single parameter, the other ones being constant and equal to those of the reference vehicle. ----, 2S-PSD:  $v = 10$  m/s; ·-·-·, 2S-PSD:  $v = 50$  m/s; —, 1S-PSD: any speed.

- (4)  $\sigma_{F_z}$  does not depend significantly on the vehicle body mass  $m_2$ ,
- (5) the suspension damping  $r_2$  has significant influence on the standard deviation  $\sigma_{F_z}$ .

Some of the above considerations can be derived by inspection of equation (14) or equation (19).

### 2.3.3. Standard deviation of suspension stroke (working space)

By inspection of Figure 5, it may be noted that

- (1)  $\sigma_{x_2-x_1}$  is not influenced by  $k_1$  and  $k_2$  for the 1S-PSD excitation,
- (2) the remarkable influence of  $m_2$  on  $\sigma_{x_2-x_1}$  is less important at high speed for the 2S-PSD excitation,
- (3)  $\sigma_{x_2-x_1}$  is strongly influenced by the suspension damping.

The above considerations can be derived by inspection of equation (16) or equation (20).

## 3. MULTI-OBJECTIVE PROGRAMMING

### 3.1. PROBLEM FORMULATION

The theory of Multi-Objective Programming (MOP) can be found in references [17, 20, 31]. Here a brief introduction on the main issues of MOP will be given, with reference to the problem of a vehicle running on rough road. Consider a system model as the one depicted in Figure 1. The relevant performance indices of the system are, as shown in the previous part of the paper, discomfort, road holding and working space. These performance indices are

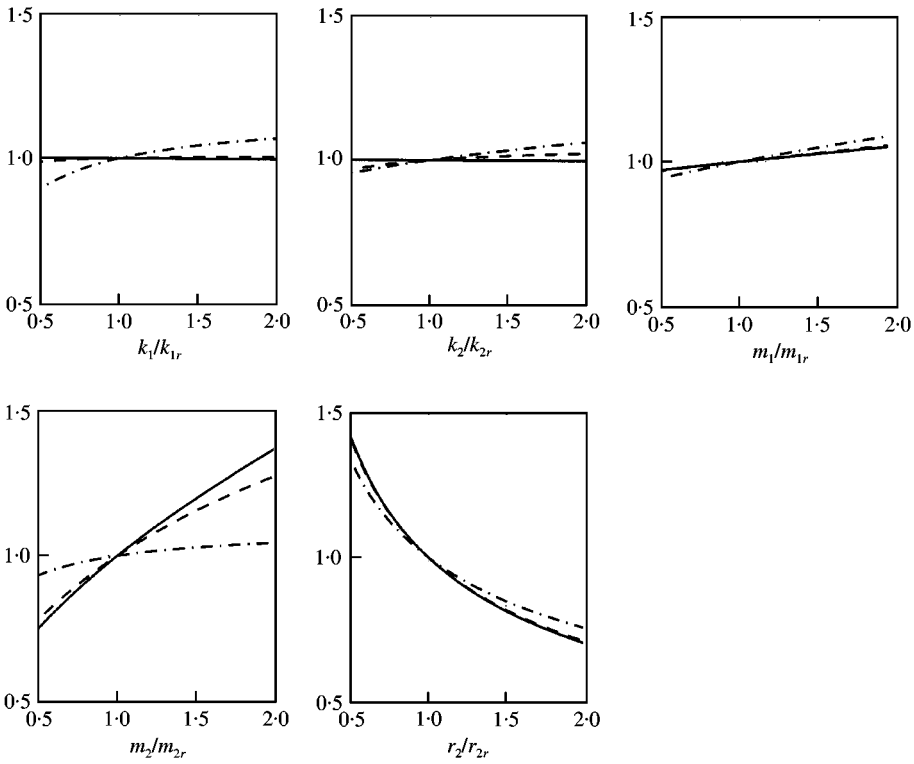


Figure 5.  $\sigma_{x_2-x_1}/\sigma_{x_2-x_1,r}$ : non-dimensional standard deviation of working space as function of model parameters. Data of the reference vehicle in Table 1, running condition data in Table 2. Each diagram has been obtained by varying one single parameter, the other ones being constant and equal to those of the reference vehicle. ----, 2S-PSD:  $v = 10$  m/s; - · - · - ·, 2S-PSD:  $v = 50$  m/s; —, 1S-PSD: any speed.

conflicting, i.e., improving one of them implies at least worsening another one. Usually, designers are interested in finding the best compromise among these performance indices by varying the system’s model parameters (e.g., suspension stiffness  $k_2$  and damping  $r_2$ ). Finding the best compromise implies, in this case, the contemporary minimization of the performance indices (often called “objective functions” or “objectives”). Thus, a vector composed of many objective functions has to be minimized. Consider the minimization of a vector composed of two objective functions, e.g., discomfort  $\bar{\sigma}_{\ddot{x}_2}^2$  and road holding  $\bar{\sigma}_{F_z}^2$ , which are assumed to be functions of suspension stiffness  $k_2$  and damping  $r_2$ . If discomfort and road holding were to be minimized separately, the suspension parameters minimizing  $\bar{\sigma}_{\ddot{x}_2}^2$  and  $\bar{\sigma}_{F_z}^2$  would read as

$$\min \bar{\sigma}_{\ddot{x}_2}^2 (k_2, r_2) \rightarrow (k_{2,\min\bar{\sigma}_{\ddot{x}_2}^2}, r_{2,\min\bar{\sigma}_{\ddot{x}_2}^2}),$$

$$\min \bar{\sigma}_{F_z}^2 (k_2, r_2) \rightarrow (k_{2,\min\bar{\sigma}_{F_z}^2}, r_{2,\min\bar{\sigma}_{F_z}^2}).$$

Obviously, there are two different vectors of parameters (namely  $k_{2,\min\bar{\sigma}_{\ddot{x}_2}^2}, r_{2,\min\bar{\sigma}_{\ddot{x}_2}^2}$  and  $k_{2,\min\bar{\sigma}_{F_z}^2}, r_{2,\min\bar{\sigma}_{F_z}^2}$ ) which minimize separately  $\bar{\sigma}_{\ddot{x}_2}^2$  and  $\bar{\sigma}_{F_z}^2$ . If  $\bar{\sigma}_{\ddot{x}_2}^2$  and  $\bar{\sigma}_{F_z}^2$  were to be minimized

contemporarily, i.e.,

$$\min \left( \begin{matrix} \bar{\sigma}_{\bar{x}_2}^2(k_2, r_2) \\ \bar{\sigma}_{\bar{r}_2}^2(k_2, r_2) \end{matrix} \right),$$

the solution would be, by definition (25), function of parameters  $k_2, r_2$

$$f(k_2, r_2) = 0.$$

There are many methods to find  $f(k_2, r_2) = 0$  (see reference [17]).

The designer should tune the suspension parameters according to the above equation. The function  $f(k_2, r_2) = 0$  will be derived below (equation (32)).

In general, a Multi-Objective Programming (MOP) problem can be formulated as

$$\min g(z) = \min \left( \begin{matrix} g_1(z_1, z_2, \dots, z_n) \\ g_2(z_1, z_2, \dots, z_n) \\ \dots \\ g_k(z_1, z_2, \dots, z_n) \end{matrix} \right), \tag{24}$$

where  $z_1, z_2, \dots, z_n$  are the  $n$  model’s parameters and  $g_1, g_2, \dots, g_k$  are the  $k$  model’s performance indices. For computational purposes, the performance indices or objective functions  $g_k$  should at least be continuous functions of the model’s parameters. The aim is to find the optimal solutions, i.e., those solutions which minimize the vector  $g(z)$  as indicated above. The model parameters ( $z$ ) may vary within a pre-defined domain  $Z$  (feasible domain). These optimal solutions are often called *efficient solutions* or *Pareto-optimal solutions*.

In a multi-objective optimization problem the “best” solutions (“Pareto-optimal” solutions) do exist and can be found by using the following definition. The solution  $z^*$  is Pareto-optimal (non-dominated) if another solution  $z$  does not exist such that

$$\begin{aligned} g_r(z) &\leq g_r(z^*), \quad r = 1, 2, 3, \dots, k, \\ \exists l: g_l(z) &< g_l(z^*). \end{aligned} \tag{25}$$

The designer will skip all dominated solutions and choose the final preferred solution among the non-dominated ones only.

Pareto-solutions are in general not unique and constitute a set. Methods to find the whole set of efficient solutions are reported in references [17, 20, 31–35].

### 3.2. CONSTRAINTS METHOD TO FIND OPTIMAL SOLUTIONS

One useful method to find Pareto-optimal solutions is the Constraints Method [17, 20, 32, 36]. It may be introduced with an example. Consider a problem in which two conflicting performance indices  $g_i$  ( $i = 1, 2$ ) and  $n$  parameters  $z_i$  appear

$$\min \left( \begin{matrix} g_1(z_1, z_2, \dots, z_n) \\ g_2(z_1, z_2, \dots, z_n) \end{matrix} \right). \tag{26}$$

By constraining the performance index  $g_2$  to a level  $\bar{g}_2$ , the problem can be transformed into the following Non-Linear Programming problem:

$$\begin{aligned} \min g_1(z_1, z_2, \dots, z_n), \\ g_2(z_1, z_2, \dots, z_n) &\leq \bar{g}_2. \end{aligned} \tag{27}$$

The values of the parameters which minimize  $g_1$  are efficient (i.e., optimal) solutions. By properly varying the value of  $\bar{g}_2$  and searching for the new minimum of  $g_1$ , it is possible to find the whole set of optimal solutions. The designer is aware of all possible choices when the whole set of optimal solutions is known.

### 3.2.1. Two performance indices

If two conflicting performance indices  $g_i$ , which are analytical functions of two system model's parameters  $z_i$  are considered, it is possible to directly apply the Constraints Method to find the analytical expressions of both the optimal performance indices and the optimal parameters, that is,

- (1)  $g_1^* = g_1^*(g_2^*)$ , i.e., the analytical expression which gives the optimal value of the performance index  $g_1$  when  $g_2$  is at its best (or *vice versa*, which is conceptually the same,  $g_2^* = g_2^*(g_1^*)$ ).
- (2)  $z_1^* = z_1^*(z_2^*)$  (or *vice versa*  $z_2^* = z_2^*(z_1^*)$ ), i.e., the analytical expression which gives the optimal values of the parameters  $z_1$  and  $z_2$  corresponding to  $g_1^*$  or  $g_2^*$ .

Being  $g_1 = g_1(z_1, z_2)$  and  $g_2 = g_2(z_1, z_2)$  the performance indices and  $z_1$  and  $z_2$  the system model's parameters, the procedure to find the analytical expressions  $g_1^* = g_1^*(g_2^*)$  and  $g_2^* = g_2^*(g_1^*)$  is the following:

- (1) from the mathematical expression  $g_1 = g_1(z_1, z_2)$  the expression  $z_2 = z_2(g_1, z_1)$  is derived by fixing the value of  $g_1$ ;
- (2) by substituting the expression derived at point 1) in the expression  $g_2 = g_2(z_1, z_2)$  the expression  $g_2 = g_2(g_1, z_1)$  is obtained;
- (3) the minimum of  $g_2$  is searched for by setting to zero the following derivative:

$$\frac{dg_2(g_1, z_1)}{dz_1} = 0$$

and checking that

$$\frac{d^2g_2(g_1, z_1)}{dz_1^2} > 0$$

this corresponds to the search for the minimum of the performance index  $g_2$ , while the performance index  $g_1$  is kept constant; from the expression of the first derivative, the expression  $z_1 = z_1(g_1)$  can be obtained;

- (4) the expression  $z_1 = z_1(g_1)$  is substituted into  $g_2 = g_2(g_1, z_1)$  and by this way it is possible to get the expression  $g_2^* = g_2^*(g_1^*)$  which defines the relationship between the two optimal performance indices;
- (5) the equation  $g_2^* = g_2^*(g_1^*)$  is the image in the plane  $(g_1-g_2)$  of the equation  $z_1^* = z_1^*(z_2^*)$  in the plane  $(z_1-z_2)$ .  $z_1^* = z_1^*(z_2^*)$  may be obtained by substitution.

### 3.2.2. Three performance indices

Before applying the Constraints Method (introduced in the previous section) to problems with more than two performance indices, Monotonicity analysis has to be applied for determining constraint activity.

The following theorems [37, 38] (Theorems of Monotonicity) apply to the problem of finding the optimal compromise between more than two performance indices.

If the performance indices and all inequality constraints (37) are globally monotonic with respect to all parameters  $z_i \in Z > 0$  then

**Theorem 1.** *If the variable  $z_i$  is explicitly represented in the performance index to be minimized, then there exists at least one active constraint with opposite monotonicity with respect to  $z_i$ .*

**Theorem 2.** *A variable  $z_i$  that is not explicitly represented in the performance index must either only be contained in constraints that are inactive, or else there must exist at least two active constraints having opposite monotonicities with respect to  $z_i$ .*

These theorems will be used in the next section.

### 3.3. OPTIMAL SUSPENSION PARAMETERS

The mathematical procedure described above has been used to optimize the parameters of the suspension of a road vehicle described by the simple system model in Figure 1. The parameters to be optimized are the stiffness  $k_2$  and the damping  $r_2$  of the suspension and the tyre radial stiffness  $k_1$ , and the performance indices are  $\sigma_{\ddot{x}_2}$  (discomfort),  $\sigma_{F_z}$  (road holding) and  $\sigma_{x_2-x_1}$  (working space).

By analyzing the expressions given by equations (14) and (12) it can be seen that both  $\sigma_{\ddot{x}_2}$  and  $\sigma_{F_z}$  increase monotonically with  $k_1$  (if reasonable variations for the suspension parameters are considered) and  $\sigma_{x_2-x_1}$  depends only on  $r_2$ . For these reasons, the problem can be simplified by considering only two parameters,  $k_2$  and  $r_2$ . The first result is that in any case the tyre radial stiffness  $k_1$  has to be kept at the lower bound of the admissible range.

The following subsections describe in detail the derivation of the Pareto-optimal set for different combinations of performance indices.

#### 3.3.1. Suspension parameters for optimal $\sigma_{\ddot{x}_2}$ , $\sigma_{F_z}$ (1S-PSD)

By applying the procedure based on the Constraints Method presented in section 3.2.1 the suspension setting for optimal  $\sigma_{\ddot{x}_2} - \sigma_{F_z}$  can be found.

Consider two parameters ( $k_1$  is kept at the minimum)  $k_2$  the suspension stiffness and  $r_2$  the damping constant.

The performance indices are  $\sigma_{\ddot{x}_2}$ , discomfort (equation (13))  $\sigma_{F_z}$ , road holding (equation (15)).

Solving equation (13) with respect to  $k_2$ , a function of  $r_2$  and  $\bar{\sigma}_{\ddot{x}_2}^2$  is obtained

$$k_2 = \sqrt{\frac{\bar{\sigma}_{\ddot{x}_2}^2 m_2^2 r_2}{(m_1 + m_2)} - \frac{k_1 r_2^2}{(m_1 + m_2)}}. \tag{28}$$

By substituting  $k_2$  in equation (15)  $\bar{\sigma}_{F_z}^2$  can be expressed as

$$\bar{\sigma}_{F_z}^2 = (m_1 + m_2)^2 \left( \bar{\sigma}_{\ddot{x}_2}^2 + \frac{k_1^2 m_1}{r_2 (m_1 + m_2)^2} - \frac{2k_1 m_1}{m_2 r_2 (m_1 + m_2)} (S_S) \right), \tag{29}$$

$$(S_S) = \sqrt{\frac{\bar{\sigma}_{\ddot{x}_2}^2 m_2^2 r_2}{(m_1 + m_2)} - \frac{k_1 r_2^2}{(m_1 + m_2)}}.$$

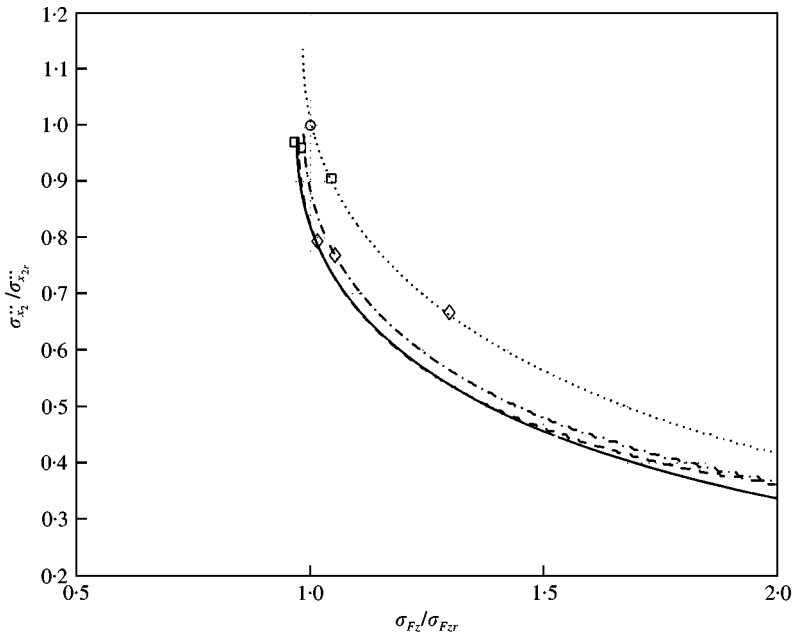


Figure 6. Pareto-optimal sets for the  $\sigma_{\ddot{x}_2}$ - $\sigma_{F_z}$  problem. Plot in non-dimensional form, vehicle data in Table 1, running condition data in Table 2. The points highlighted by using special symbols ( $\diamond$ ,  $\square$ ) refer to the points in Figure 7. ----, 2S-PSD:  $v = 1$  m/s; ·····, 2S-PSD:  $v = 10$  m/s; ······, 2S-PSD: 50 m/s; —, 1S-PSD: any speed;  $\circ$ , ref. vehicle.

The minimum of equation (29) is now computed by setting to zero the first derivative with respect to  $r_2$

$$\frac{d\bar{\sigma}_{F_z}}{dr_2} = 0 \rightarrow r_2 = \frac{k_1^2 m_2^2 \bar{\sigma}_{\ddot{x}_2}^2}{m_2^2 (\bar{\sigma}_{\ddot{x}_2}^2)^2 (m_1 + m_2) + k_1^3}. \tag{30}$$

By substituting  $r_2$  in equation (29) the relationship between optimal  $\sigma_{\ddot{x}_2}$  and optimal  $\sigma_{F_z}$  can be obtained (see Figure 6)

$$\bar{\sigma}_{F_z}^{*2} = m_2(m_1 + m_2) \bar{\sigma}_{\ddot{x}_2}^{*2} + \frac{m_1 k_1^3}{m_2^2 \bar{\sigma}_{\ddot{x}_2}^{*2}}, \tag{31}$$

$$2\sqrt{\frac{m_1 k_1^3 (m_1 + m_2)}{m_2}} < \bar{\sigma}_{F_z}^{*2} < \infty, \quad \sqrt{\frac{m_1 k_1^3}{(m_1 + m_2) m_2^3}} > \bar{\sigma}_{\ddot{x}_2}^{*2} > 0,$$

the corresponding expression in the optimal parameter domain (Figure 7) reads as

$$k_2^* = \sqrt{\frac{m_2 k_1}{(m_1 + m_2)} \left( \frac{m_2 k_1}{(2m_1 + m_2)} - \frac{r_2^{*2}}{m_2} - \frac{\sqrt{k_1^2 m_2^2 - 4k_1 r_2^{*2} (m_1 + m_2)}}{2(m_1 + m_2)} \right)}. \tag{32}$$

The last equation has been obtained by substituting equations (13) and (15) into equation (31).

It is important to note that equation (31), if taken without the constraints referring to  $\bar{\sigma}_{\ddot{x}_2}^{*2}$  and  $\bar{\sigma}_{F_z}^{*2}$ , defines both Pareto-optimal solutions and non-Pareto-optimal solutions. This

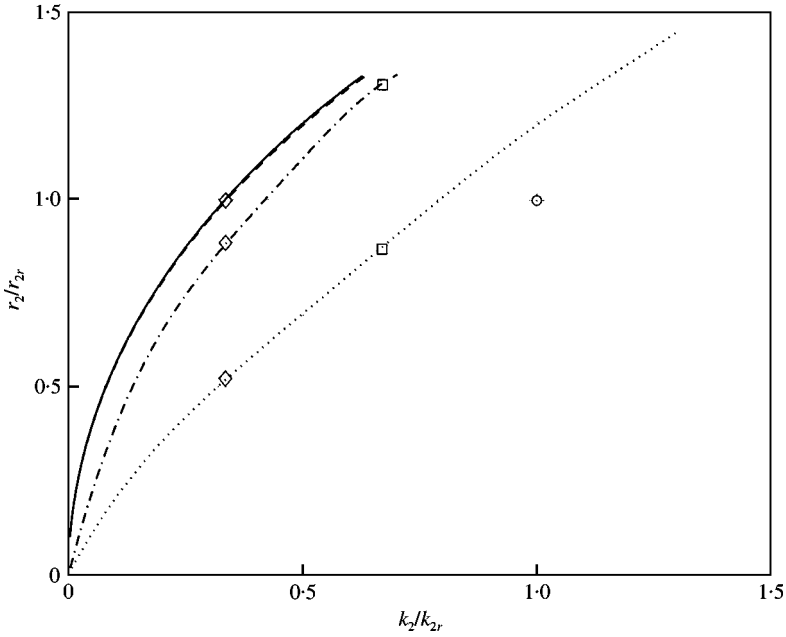


Figure 7. Pareto-optimal sets (parameters domain) for the  $\sigma_{x_2}$ - $\sigma_{F_z}$  problem. Plot in non-dimensional form, vehicle data in Table 1, running condition data in Table 2. The points highlighted by using special symbols ( $\diamond$ ,  $\square$ ) refer to the points in Figure 6. - - - - , 2S-PSD:  $v = 1$  m/s; - · - · - · , 2S-PSD:  $v = 10$  m/s; · · · · · , 2S-PSD:  $v = 50$  m/s; —, 1S-PSD: any speed;  $\circ$ , ref. vehicle.

is due to the particular implementation of the Constraints Method employed (see section 3.2.1). Thus, in order to compute correctly the Pareto-optimal set, the inequalities have to be considered. The lower and upper bounds in equations (31) define the extrema ( $g_1(\min)$ ,  $g_2(g_1(\min))$  and  $g_1(g_2(\min))$ ,  $g_2(\min)$ ) represented in Figure 8, corresponding to the two solutions that minimize one by one the two performance indices  $g_1 = \bar{\sigma}_{F_z}^2$  and  $g_2 = \bar{\sigma}_{x_2}^2$ . The two extrema of the Pareto-optimal set can be obtained as follows. The minimum of  $\bar{\sigma}_{x_2}^2$  is obtained by setting  $\partial \bar{\sigma}_{x_2}^2 / \partial r_2 = 0$ ,  $\partial \bar{\sigma}_{x_2}^2 / \partial k_2 = 0$ , so  $g_2(\min) = \bar{\sigma}_{x_2}^2(\min) = 0$  (the corresponding  $g_1(g_2(\min)) = \bar{\sigma}_{F_z}^2 = \infty$  (see equation (31)) as shown in Figure 8. The minimum of  $\bar{\sigma}_{F_z}^2$  is derived by setting  $\partial \bar{\sigma}_{F_z}^2 / \partial r_2 = 0$ ,  $\partial \bar{\sigma}_{F_z}^2 / \partial k_2 = 0$ , so

$$g_1(\min) = \bar{\sigma}_{F_z}^2(\min) = 2 \sqrt{\frac{m_1 k_1^3 (m_1 + m_2)}{m_2}}$$

and the corresponding

$$g_2(g_1(\min)) = \bar{\sigma}_{x_2}^2 = \sqrt{\frac{m_1 k_1^3}{(m_1 + m_2) m_2^3}}$$

3.3.2. Suspension parameters for optimal  $\sigma_{x_2}$ ,  $\sigma_{x_2-x_1}$  (1S-PSD)

The equation that defines the Pareto-optimal set for the discomfort—working space problem (Figure 9) is

$$\bar{\sigma}_{x_2}^{*2} = \frac{k_1(m_1 + m_2)}{m_2^2 \bar{\sigma}_{x_2-x_1}^{*2}} \tag{33}$$



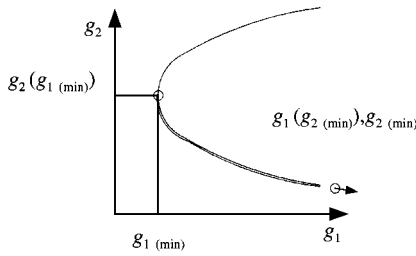


Figure 8. Limitations on the curve that contains the Pareto-optimal set. The points highlighted by circles (O) identify the Pareto-optimal set on the curve derived by applying the Constraints Method.

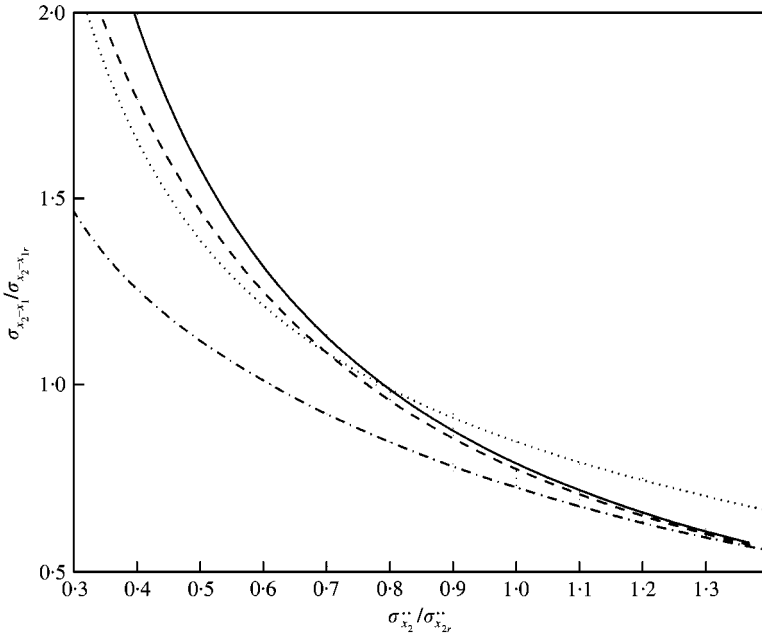


Figure 9. Pareto-optimal sets for the  $\sigma_{x_2} - \sigma_{x_2-x_1}$  problem. Plot in non-dimensional form, vehicle data in Table 1, running condition data in Table 2. ---, 2S-PSD:  $v = 1$  m/s; - · - · - ·, 2S-PSD:  $v = 10$  m/s; ·····, 2S-PSD:  $v = 50$  m/s; —, 1S-PSD: any speed; ○, ref. vehicle.

Equation (33) has been obtained as shown in section 3.2.1. Equation (33) contains the whole Pareto-optimal set being  $g_2(\min) = \bar{\sigma}_{x_2}^2(\min) = 0$  (corresponding to  $g_1(g_2(\min)) = \bar{\sigma}_{x_2-x_1}^2 = \infty$ ) and  $g_1(\min) = \bar{\sigma}_{x_2-x_1}^2(\min) = 0$  (corresponding to  $g_2(g_1(\min)) = \bar{\sigma}_{x_2}^2 = \infty$ ).

The equation of the Pareto-optimal set into the parameter space is

$$k_2^* = 0. \tag{34}$$

So, the Pareto-optimal set is the  $r_2$ -axis.

### 3.3.3. Suspension parameters for optimal $\sigma_{x_2-x_1}$ , $\sigma_{F_z}$ (1S-PSD)

By applying again the procedure presented in section 3.2.1. the Pareto-optimal set for the road holding—working space problem ( $\sigma_{F_z}$ ,  $\sigma_{x_2-x_1}$ ) can be derived (Figure 10).

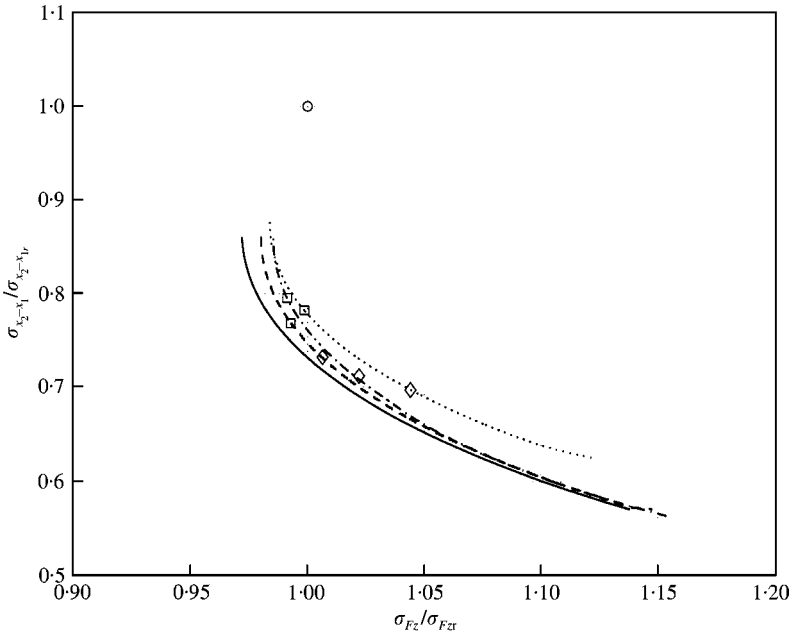


Figure 10. Pareto-optimal sets for the  $\sigma_{x_2-x_1}, \sigma_{F_z}$  problem. Plot in non-dimensional form, vehicle data in Table 1, running condition data in Table 2. The points highlighted by using special symbols ( $\diamond$ ,  $\square$ ) refer to the points in Figure 11. ---, 2S-PSD:  $v = 1$  m/s; ·····, 2S-PSD:  $v = 10$  m/s; ······, 2S-PSD:  $v = 50$  m/s; —, 1S-PSD: any speed;  $\circ$ , ref. vehicle.

$$\bar{\sigma}_{F_z}^{*2} = \frac{m_1 k_1^2 \bar{\sigma}_{x_2-x_1}^{*2}}{m_1 + m_2} - \frac{m_1^2 k_1^2 \bar{\sigma}_{x_2-x_1}^{*2}}{(m_1 + m_2)^2} + \frac{k_1 (m_1 + m_2)^3}{m_2^2 \bar{\sigma}_{x_2-x_1}^{*2}}, \tag{35}$$

$$2 \sqrt{\frac{m_1 k_1^3 (m_1 + m_2)}{m_2}} < \bar{\sigma}_{F_z}^{*2} < \infty, \quad \sqrt{\frac{(m_1 + m_2)^5}{m_1 m_2^3 k_1}} > \bar{\sigma}_{x_2-x_1}^2 > 0.$$

The bounds of the inequalities can be obtained by computing the minimum of working space  $g_2(\min) = \bar{\sigma}_{x_2-x_1}^2(\min) = 0$  (corresponding to  $g_1(g_2(\min)) = \bar{\sigma}_{F_z}^2 = \infty$ , see Figure 8) and the minimum of the road holding  $g_1(\min) = \bar{\sigma}_{F_z}^2(\min) = 2 \sqrt{\frac{m_1 k_1^3 (m_1 + m_2)}{m_2}}$ ,  $g_2(g_1(\min)) = \bar{\sigma}_{x_2-x_1}^2 = \sqrt{\frac{(m_1 + m_2)^5}{m_1 m_2^3 k_1}}$ .

The Pareto-optimal set in the parameter domain is

$$k_2^* = \frac{m_1 m_2 k_1}{(m_1 + m_2)^2}. \tag{36}$$

The Pareto-optimal set is the line parallel to the  $r_2$ -axis (Figure 11).

3.3.4. Suspension parameters for optimal  $\sigma_{\ddot{x}_2}, \sigma_{F_z}, \sigma_{x_2-x_1}$  (1S-PSD)

The MOP problem can be reformulated by using the Constraints Method [20, 17, 32] as

$$\begin{aligned} \min \sigma_{x_2-x_1}^2 &= g_1(r_2) && \text{equations (16, 17),} \\ \sigma_{F_z}^2 &= g_2(r_2, k_2) \leq \bar{g}_2 && \text{equations (14, 15),} \\ \sigma_{\ddot{x}_2}^2 &= g_3(r_2, k_2) \leq \bar{g}_3 && \text{equations (12, 13),} \end{aligned} \tag{37}$$

( $k_1$  is not considered because it should be kept always at its minimum value).

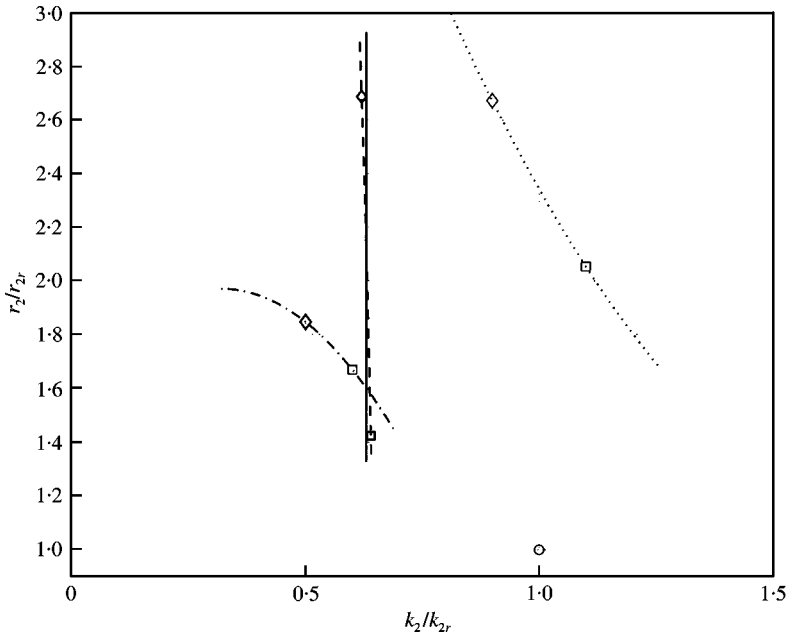


Figure 11. Pareto-optimal sets (parameters domain) for the  $\sigma_{x_2-x_1}-\sigma_{F_z}$  problem. Plot in non-dimensional form, vehicle data in Table 1, running condition data in Table 2. The points highlighted by using special symbols ( $\diamond$ ,  $\square$ ) refer to the points in Figure 10. ----, 2S-PSD:  $v = 1$  m/s; - · - · - ·, 2S-PSD:  $v = 10$  m/s; ·····, 2S-PSD: 50 m/s; —, 1S-PSD: any speed;  $\circ$ , ref. vehicle.

The variable  $k_2$  is not explicitly represented in the performance index  $g_1$ . According to the Theorem 2 (section 3.2.2) at least two active constraints having opposite monotonicities with respect to  $k_2$  must exist. So the two inequalities constraints in equation (37) are active (i.e., the equality holds) and problem (37) is reduced to the solution of

$$\begin{aligned} \sigma_{x_2-x_1}^2 &= g_1(r_2), \\ \sigma_{F_{z1}}^2 &= g_2(r_2, k_2), \\ \sigma_{\ddot{x}_2}^2 &= g_3(r_2, k_2). \end{aligned} \tag{38}$$

The analytical expression of the surface which contains the Pareto-optimal set in the  $\sigma_{\ddot{x}_2}, \sigma_{F_{z1}}, \sigma_{x_2-x_1}$  domain is derived from equation (38) by eliminating  $k_2, r_2$ .

$$\bar{\sigma}_{F_z}^{*2} = \bar{\sigma}_{\ddot{x}_2}^{*2} (m_2 + m_1)^2 + \frac{m_1 k_1^2}{(m_2 + m_1)} \bar{\sigma}_{x_2-x_1}^{*2} - \frac{2m_1 k_1}{m_2} (Q), \tag{39}$$

$$Q = \sqrt{\bar{\sigma}_{\ddot{x}_2}^{*2} m_2^2 \bar{\sigma}_{x_2-x_1}^{*2} - k_1 (m_2 + m_1)}.$$

The corresponding Pareto-optimal parameters ( $k_2, r_2$ ) can be readily calculated

$$r_2^* = \frac{m_2 + m_1}{\bar{\sigma}_{x_2-x_1}^{*2}}, \tag{40}$$

$$k_2^* = \frac{\sqrt{\bar{\sigma}_{\ddot{x}_2}^{*2} m_2^2 \bar{\sigma}_{x_2-x_1}^{*2} - k_1 (m_2 + m_1)}}{\bar{\sigma}_{x_2-x_1}^{*2}}. \tag{41}$$

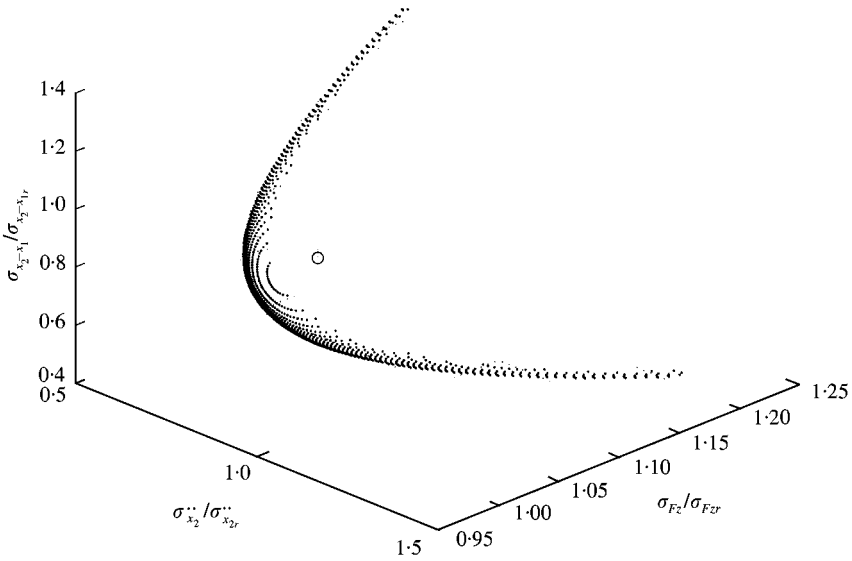


Figure 12. Pareto-optimal set in the discomfort ( $\sigma_{\ddot{x}_2}$ )–road-holding ( $\sigma_{F_z}$ )–working-space ( $\sigma_{x_2-x_1}$ ) domain. Plot in non-dimensional form, vehicle data in Table 1, running condition data in Table 2. The 1S-PSD is considered. The reference vehicle is represented by the small circle.

It may be noted that  $r_2^*, k_2^*$  do not depend on  $A_b \cdot v$ ; i.e., the optimal parameter settings do not depend on vehicle speed.

The Pareto-optimal set, defined by equation (39), is plotted in the  $\sigma_{\ddot{x}_2}, \sigma_{F_{z1}}, \sigma_{x_2-x_1}$  space (performance indexes space) in Figure 12. Geometrically, in this case (three-dimensional space), the Pareto-optimal set is a surface. Figure 13 shows the projection of the Pareto-optimal set (surface) depicted in Figure 12 on to the three planes ( $\sigma_{F_{z1}}, \sigma_{x_2-x_1}$ ), ( $\sigma_{\ddot{x}_2}, \sigma_{F_{z1}}$ ) and ( $\sigma_{\ddot{x}_2}, \sigma_{x_2-x_1}$ ). The Pareto-optimal sets in the parameters domain ( $k_2, r_2$ ) are shown in Figure 14.  $k_1$  is kept always at its minimum value.

The Pareto-optimal sets related to the problem formulated by considering only two performance indices (sections 3.3.1, 3.3.2, 3.3.3) are obviously on the border of the projection on to a bi-dimensional domain (plane) of the surface which represents the Pareto-optimal set related to the problem with three performance indices. Moreover, they constitute the boundaries of the Pareto-optimal surface.

3.3.5. Suspension parameters for optimal  $\sigma_{\ddot{x}_2}, \sigma_{F_z}$  (2S-PSD)

When the road irregularity is defined by the 2S-PSD, the analytical derivation of the Pareto-optimal set is rather impractical. So the Pareto-optimal set has been computed numerically, i.e.,  $k_2$  and  $r_2$  have been varied and the response of the model in terms of  $\sigma_{\ddot{x}_2}$  (equation (18)) and  $\sigma_{F_z}$  (equation (19)) has been computed. The Pareto-optimal solutions have been selected by directly applying the Pareto-optimality definition (25). The approximated Pareto-optimal set is plotted in Figure 6 into the performance indices domain and in Figure 7 into the parameters domain. Three different vehicle speeds (1, 10, 50 m/s) have been considered.

The relationship between  $k_2$  and  $r_2$  is different with respect to the case 1S-PSD as the vehicle speed increases (see Figure 11).

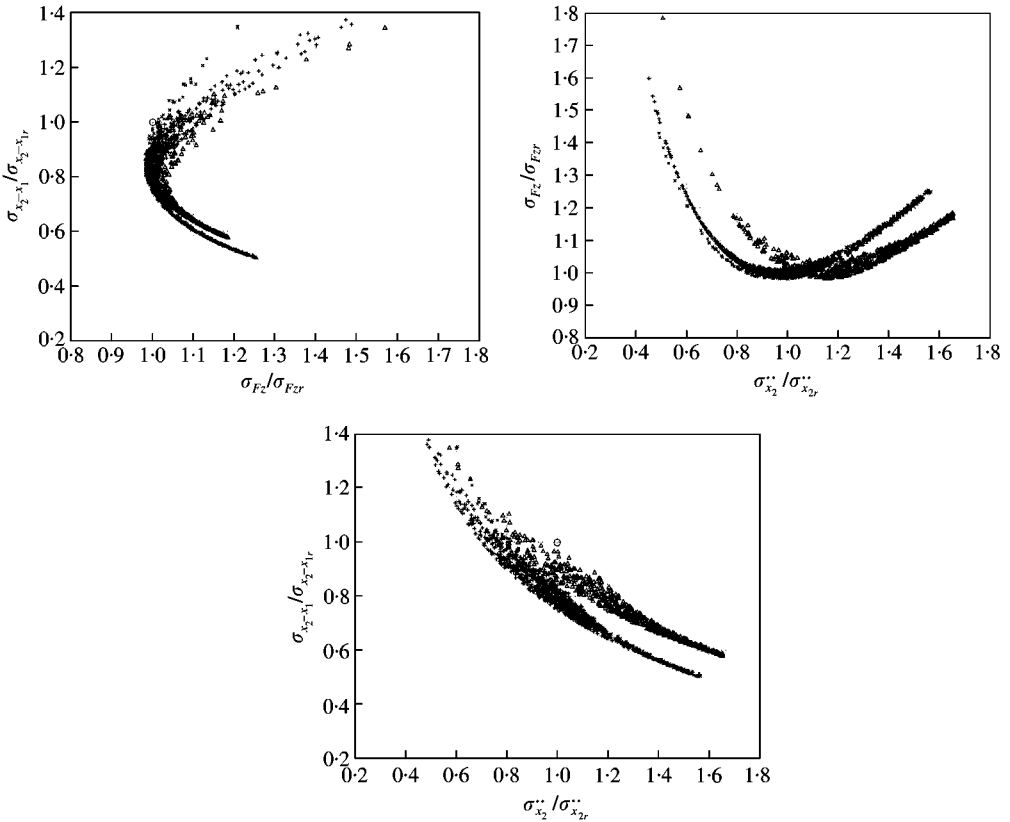


Figure 13. Projection of the Pareto-optimal set shown in Figure 12 in the discomfort ( $\sigma_{\ddot{x}_2}$ ) road-holding ( $\sigma_{F_z}$ ) working-space ( $\sigma_{x_2-x_1}$ ) domain. Bi-dimensional projections. Plot in non-dimensional form, vehicle data in Table 1, running condition data in Table 2.  $\times$ , 2S-PSD: 1 m/s;  $+$ , 2S-PSD: 10 m/s;  $\Delta$ , 2S-PSD: 50 m/s;  $\circ$ , ref. vehicle.

3.3.6. Suspension parameters for optimal  $\sigma_{\ddot{x}_2}$ ,  $\sigma_{x_2-x_1}$  (2S-PSD)

The numerical procedure introduced in section 3.3.5 has been used to compute the Pareto-optimal set referring to  $\sigma_{\ddot{x}_2}$  and  $\sigma_{x_2-x_1}$ . The Pareto-optimal set is shown in Figure 9. Three different vehicle speeds (1, 10, 50 m/s) have been considered.

The shape of the curve (Figure 9) that represents the Pareto-optimal set  $\sigma_{\ddot{x}_2} - \sigma_{x_2-x_1}$  is different from the curve obtained by considering the 1S-PSD, in this case the effect of the modified road irregularity spectrum is less important with respect to the  $\sigma_{\ddot{x}_2}$ ,  $\sigma_{F_z}$  case.

3.3.7. Suspension parameters for the optimal  $\sigma_{x_2-x_1} - \sigma_{F_z}$  (2S-PSD)

The Pareto-optimal set considering  $\sigma_{x_2-x_1}$  and  $\sigma_{F_z}$  is shown in Figure 10 (parameters domain) and Figure 11 (performance indices domain). Three different vehicle speeds (1, 10, 50 m/s) have been considered.

The relationship between  $k_2$  and  $r_2$  is different with respect to the case 1S-PSD (Figure 11). This is due to the fact that  $\sigma_{x_2-x_1}$  does not depend on  $k_2$  when a road described by the 1S-PSD irregularity is considered.

3.3.8. Suspension parameters for optimal  $\sigma_{\ddot{x}_2} - \sigma_{F_z} - \sigma_{x_2-x_1}$  (2S-PSD)

A numerical search algorithm has been designed [34] and used to approximate the Pareto-optimal set considering three performance indices, namely  $\sigma_{\ddot{x}_2}$ ,  $\sigma_{F_z}$ , and  $\sigma_{x_2-x_1}$ . The

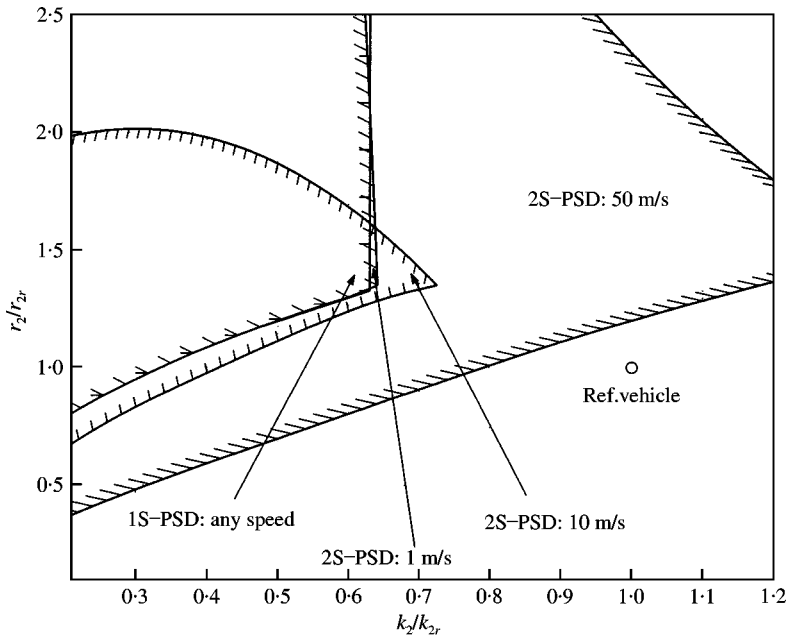


Figure 14. Images of the Pareto-optimal set plotted in Figure 13 onto the  $k_2$ - $r_2$  parameter domain. Plot in non-dimensional form, vehicle data in Table 1, running condition data in Table 2. The optimal  $k_2$ ,  $r_2$  must lay within the indicated boundaries. The reference vehicle is not optimal within the speed range 1-50 m/s.

projections of the Pareto-optimal surface on to the performance index domain are shown in Figure 13. The corresponding parameters are limited by the lines plotted in Figure 14. Again three different vehicle speeds (1, 10, 50 m/s) have been considered.

#### 4. CONCLUSION

Simple analytical formulae have been derived symbolically in order to describe the response of vehicles to random excitation generated by the vertical road irregularity. Two different road irregularity spectra have been considered (1S-PSD and 2S-PSD). The analytical formulae should estimate with reasonable accuracy the dynamic behaviour of an actual road vehicle running on rough road. On the basis of the derived analytical formulae, a parameter sensitivity analysis has been performed with reference to relevant performance indices, namely the standard deviations of the body acceleration (discomfort), of the vertical force on the wheel (road holding), of the suspension stroke (working space).

Depending on the power spectral density of the road irregularity (1S-PSD or 2S-PSD) and on the vehicle speed, the sensitivity of performance indices to suspension parameters variations may dramatically change. This happens for example, referring to the influence of the suspension stiffness on road holding, of the damping ratio on discomfort, of the body mass on working space.

In the second part of the paper, by using the derived analytical formulae, a theoretically rigorous method, based on Multi-Objective Programming (MOP) and Monotonicity analysis, has been applied to find the best trade-off for conflicting performance indices such as discomfort, road holding and working space.

In case the excitation is given by a simplified road spectrum irregularity (1S-PSD), simple analytical formulae have been derived symbolically for the optimal compromise among

discomfort, road holding and working space. Correspondingly, the optimal suspension damping and the optimal tyre and suspension stiffnesses have also been derived symbolically.

If the excitation is defined by the simple road spectrum (1S-PSD) the optimal suspension settings do not depend on vehicle speed. The opposite occurs when considering the (2S-PSD) excitation spectrum. The best compromise between discomfort and road holding is obtained by increasing (or decreasing) both the suspension stiffness and damping. The relationship between stiffness and damping depends strongly on the vehicle speed if the best compromise between road holding and working space has to be obtained.

When discomfort, road holding and working space have to be optimized contemporarily, the optimal suspension parameters (stiffness and damping) have to be set within well-defined ranges which have been derived (numerically) in the paper. The tyre radial stiffness has always to be kept at its minimum value.

Some of the above conclusions are partially understood from road vehicle dynamics research. The main contribution of the paper is the provision, in a rigorous way, and (whenever possible) in analytical form, of the basic equations for describing and optimizing the dynamic behaviour of vehicles running on randomly profiled roads.

## REFERENCES

1. P. MUELLER and W. SCHIEHLEN 1985 *Linear Vibrations* Dordrecht: Martinus Nijhoff.
2. D. HROVAT 1993 *Transactions of the American Society of Mechanical Engineers, Journal of Dynamic Systems, Measurement, and Control* **115**, 328–342. Applications of optimal control to advanced automotive suspension design.
3. R. CHALASANI 1983 *Internal Report General Motor Research Laboratories*. Ride performance potential of active suspension systems.
4. A. THOMPSON 1983 *SAE Paper* 830663. Suspension design for optimum road holding.
5. X. LU and AL. 1984 *International Journal of Vehicle Design* **5**, 129–141. A design procedure for optimization of vehicle suspensions.
6. G. MASTINU 1988 *Technical Report. Politecnico di Milano*. Escursione della sospensione dell'autoveicolo: derivazione analitica della risposta in presenza di eccitazione stocastica.
7. C. DODDS and J. ROBSON 1973 *Journal of Sound and Vibration* **31**, 175–183. The description of road surface roughness.
8. R. SHARP and D. CROLLA 1987 *Vehicle System Dynamics*, **16**, 167–192. Road vehicle suspension system design—a review.
9. M. MITSCHKE 1990 *Dynamik der Kraftfahrzeuge*. Berlin: Springer-Verlag.
10. G. MASTINU 1988 *Proceedings of the IMechE Conference—Advanced Suspensions, Institution of Mechanical Engineers, London*. Passive automobile suspension parameter adaptation.
11. T. GILLESPIE 1992 *Fundamentals of Vehicle Dynamics*. Warrendale, PA: Society of Automotive Engineering.
12. G. GENTA 1989 *Meccanica dell'autoveicolo*. Torino: Levrotto & Bella.
13. A. MORELLI 1999 *Progetto dell'autoveicolo, concetti di base*. CELID.
14. J. DIXON 1991 *Tyres, Suspension and Handling*. Cambridge: Cambridge University Press.
15. C. BOURCIER DE CARBON 1950 *Proceedings of the S.I.A. Conference, Paris*. Théorie Mathématique et Réalisation Pratique de la Suspension Amortié des Vehicules Terrestres.
16. G. MASTINU and M. GOBBI 1999 Advances in the optimal design of mechanical systems. *Technical Report, Course coordinated by CISM, International Centre for Mechanical Sciences*, web: [www.europeindia.org](http://www.europeindia.org), Birla Science Centre, Hyderabad.
17. K. MIETTINEN 1999 *Nonlinear Multiobjective Optimization*. Boston: Kluwer Academic Publishers.
18. D. GRIERSON and P. HAJELA, editors, 1996 *Emergent Computing Methods in Engineering Design—Applications of Genetic Algorithms and Neural Networks* Berlin: Springer.
19. D. SEN and J. YANG 1998 *Multiple Criteria Support in Engineering Design*. Berlin: Springer.
20. H. ESCHENAUER, J. KASKI and A. OSYCZKA, editors, 1990 *Multicriteria Design Optimization*. Berlin: Springer-Verlag.
21. G. MASTINU 1994 *Proceedings of the International Symposium on Advanced Vehicle Control AVEC94, JSAE 9438051*, 73–78. Automotive suspension design by multi-objective programming.

22. G. MASTINU 1995 in *Smart Vehicles* (J. Pauwelussen and H. Pacejka, editor) 219–251. Delft: Swets & Zeitlinger. Integrated controls and interactive multi-objective programming for the improvement of ride and handling of road vehicles.
23. M. GOBBI and AL. 2000 *Vehicle System Dynamics, Supplement 33*, 3–22. Optimal & robust design of a road vehicle suspension system.
24. M. GOBBI, G. MASTINU and C. DONISELLI 1997 *Proceedings of the 6th EAEC International Conference*, EAEC Cernobbio, Italy. Advances in the optimal design of vehicle subsystems.
25. M. GOBBI and G. MASTINU 1999 *Innovations in Vehicle Design and Development, ASME DE-Vol. 10*, 15–24. Global approximation: performance comparison of different methods, with application to road vehicle system engineering.
26. M. GOBBI, G. MASTINU and C. DONISELLI 1999 *Vehicle System Dynamics 32*, 149–170. Optimising a car chassis.
27. C. SMITH, D. M. GEHEE and A. HEALEY 1978 *Transactions of the American Society of Mechanical Engineers, Journal of Dynamic Systems, Measurement, and Control 100*, 34–41. The prediction of passenger riding comfort from acceleration data.
28. K. KAMASH and J. D. ROBSON 1978 *Journal of Sound and Vibration, 57*, 89–100. The application of isotropy in road surface modelling.
29. P. VENHOVENS 1994 *Ph.D. Thesis, Delft University of Technology, Delft, The Netherlands*. Optimal control of vehicle suspensions.
30. C. NEWTON and AL. 1957 *Analytical Design of Linear Feedback Controls, Appendix E*. New York: Wiley.
31. J. MATUSOV 1995 *Multicriteria Optimization and Engineering*. New York: Chapman & Hall.
32. W. STADLER 1988 *Multicriteria Optimization in Engineering and in the Sciences*. New York: Plenum Press.
33. R. STATNIKOV and J. MATUSOV 1996 *Journal of Optimization Theory and Applications 91*, 543–560. Use of  $\pi$ -nets for the approximation of the edgeworth-pareto set in multicriteria optimization.
34. M. GOBBI 2000 *Technical Report, Politecnico de Milano*. Approximation of the Pareto-optimal set in multi-objective optimisation.
35. P. KAMAT 1993, Editor: *Structural Optimization: Status and Promise*. Washington: AIAA.
36. W. STADLER 1995 *Microcomputers in Civil Engineering 10*, 291. Caveats and boons of multicriteria optimization.
37. N. MICHELENA and A. AGOGINO 1988 *Journal of Mechanisms, Transmissions, and Automation in Design—Transactions of the American Society of Mechanical Engineers 110*, 81–87. Multiobjective hydraulic cylinder design.
38. P. Y. PAPALAMBROS and D. J. WILDE 1991 *Principles of Optimal Design*. Cambridge: Cambridge University Press.

#### APPENDIX A: TABULATED VALUES OF THE INTEGRAL FORM

The tabulated values of  $I_k$  for  $k = 4$  and 5 reported in reference [30] are as follows

$$I_k = \frac{1}{2\pi} \int_{-\infty}^{+\infty} \frac{N(j\omega)N(-j\omega)}{D(j\omega)D(-j\omega)} ds,$$

where

$$N(j\omega) = n_{k-1}(j\omega)^{k-1} + \dots + n_0,$$

$$D(j\omega) = d_k(j\omega)^k + \dots + d_0.$$

$I_4(k = 4)$  reads as

$$I_4 = \frac{(n_3^2 c_m + (n_2^2 - 2n_1 n_3) d_0 d_1 d_4 + (n_1^2 - 2n_0 n_2) d_0 d_3 d_4 + n_0^2 (-d_1 d_4^2 + d_2 d_3 d_4))}{2d_0 d_4 (-d_0 d_3^2 - d_1^2 d_4 + d_1 d_2 d_3)},$$



where

$$c_m = -d_0^2 d_3 + d_0 d_1 d_2.$$

$I_5(k=5)$  reads as

$$I_5 = \frac{(n_4^2 c_{m0} + (n_3^2 - 2n_2 n_4) c_{m1} + n_{m0} c_{m2} + (n_1^2 - 2n_0 n_2) c_{m3} + n_0^2 c_{m4})}{2d_0(d_1 c_{m4} - d_3 c_{m3} + d_5 c_{m2})},$$

where

$$n_{m0} = n_2^2 - 2n_1 n_3 + 2n_0 n_4,$$

$$c_{m0} = 1/d_5(d_3 c_{m1} - d_1 c_{m2}),$$

$$c_{m1} = -d_0 d_3 + d_1 d_2,$$

$$c_{m2} = -d_0 d_5 + d_1 d_4,$$

$$c_{m3} = 1/d_0(d_2 c_{m2} - d_4 c_{m1}),$$

$$c_{m4} = 1/d_0(d_2 c_{m3} - d_4 c_{m2}).$$

## APPENDIX B: NOMENCLATURE

$\omega$	circular frequency, rad/s
$j$	$j = \sqrt{-1}$
$s_c$	reference circular frequency $s_c = av$ (2S-PSD), rad/s
$a$	break wave number (2S-PSD), rad/m
$\zeta$	imposed displacement, m
$A_b$	road irregularity parameter (1S-PSD), m
$A_v$	road irregularity parameter (2S-PSD), m <sup>2</sup>
$H_1$	transfer function between $\zeta$ and $\ddot{x}_2$ , 1/s <sup>2</sup>
$H_2$	transfer function between $\zeta$ and $F_{z1}$ , N/m
$H_3$	transfer function between $\zeta$ and $x_2 - x_1$ , dimensionless
$S$	power spectral density (PSD)
$v$	vehicle speed, m/s
$k_1$	tyre radial stiffness, N/m
$k_2$	suspension stiffness, N/m
$r_2$	suspension damping, Ns/m
$m_1$	unsprung mass, kg
$m_2$	sprung mass, kg
$x_1$	mass $m_1$ absolute vertical displacement, m
$x_2$	mass $m_2$ absolute vertical displacement, m
$\sigma_{F_z}$	standard deviation of the road/wheel vertical force (road holding), N
$\sigma_{\ddot{x}_2}$	standard deviation of the body acceleration (discomfort), m/s <sup>2</sup>
$\sigma_{x_2 - x_1}$	standard deviation of the suspension stroke (working space), m
1S-PSD	one slope PSD (equation (7))
2S-PSD	two slope PSD (equation (8))
*	superscript indicating, Pareto-optimal performance index or parameter